Temperature and salinity correction coefficients for light absorption by water in the visible to infrared spectral region

Rüdiger Röttgers,[1,*] David McKee,[2] and Christian Utschig[1]

[1]*Remote Sensing Department, Institute for Coastal Research, Helmholtz-Zentrum Geesthacht, Center for Materials and Coastal Research, Geesthacht, Germany*
[2]*Physics Department, University of Strathclyde, Glasgow, Scotland, UK*
[*]*rroettgers@hzg.de*

Abstract: The light absorption coefficient of water is dependent on temperature and concentration of ions, i.e. the salinity in seawater. Accurate knowledge of the water absorption coefficient, a, and/or its temperature and salinity correction coefficients, Ψ_T and Ψ_S, respectively, is essential for a wide range of optical applications. Values are available from published data only at specific narrow wavelength ranges or at single wavelengths in the visible and infrared regions. Ψ_T and Ψ_S were therefore spectrophotometrically measured throughout the visible, near, and short wavelength infrared spectral region (400 to ~2700 nm). Additionally, they were derived from more precise measurements with a point-source integrating-cavity absorption meter (PSICAM) for 400 to 700 nm. When combined with earlier measurements from the literature in the range of 2600 – 14000 nm (wavenumber: 3800 – 700 cm^{-1}), the coefficients are provided for 400 to 14000 nm (wavenumber: 25000 to 700 cm^{-1}).

OCIS codes: (010.0010) Atmospheric and oceanic optics; (010.1030) Absorption; (010.4450) Oceanic optics; (010.7340) Water.

References and links

1. R. Lemus, "Vibrational excitations in H_2O in the framework of the local model," J. Mol. Spectrosc. **225**(1), 73–92 (2004).
2. http://www1.lsbu.ac.uk
3. D. Eisenberg and W. Kauzmann, *The Structure and Properties of Water* (Oxford University, 2005).
4. B. Woźniak and J. Dera, *Light Absorption in Sea Water* (Springer, 2007).
5. W. S. Pegau, D. Gray, and J. R. V. Zaneveld, "Absorption and attenuation of visible and near-infrared light in water: dependence on temperature and salinity," Appl. Opt. **36**(24), 6035–6046 (1997).
6. J. M. Sullivan, M. S. Twardowski, J. R. V. Zaneveld, C. M. Moore, A. H. Barnard, P. L. Donaghay, and B. Rhoades, "Hyperspectral temperature and salt dependencies of absorption by water and heavy water in the 400-750 nm spectral range," Appl. Opt. **45**(21), 5294–5309 (2006).
7. R. Röttgers and R. Doerffer, "Measurements of optical absorption by chromophoric dissolved organic matter using a point-source integrating-cavity absorption meter," Limnol. Oceanogr. Methods **5**, 126–135 (2007).
8. X. Zhang and L. Hu, "Estimating scattering of pure water from density fluctuation of the refractive index," Opt. Express **17**(3), 1671–1678 (2009).
9. X. Zhang and L. Hu, "Scattering by pure seawater at high salinity," Opt. Express **17**(15), 12685–12691 (2009).
10. X. Zhang, L. Hu, and M.-X. He, "Scattering by pure seawater: effect of salinity," Opt. Express **17**(7), 5698–5710 (2009).
11. X. Zhang, L. Hu, M. S. Twardowski, and J. M. Sullivan, "Scattering by solutions of major sea salts," Opt. Express **17**(22), 19580–19585 (2009).
12. J. R. Collins, "Change in the infrared absorption spectrum of water with temperature," Phys. Rev. **26**(6), 771–779 (1925).
13. W. S. Pegau and J. R. V. Zaneveld, "Temperature-dependent absorption of water in the red and near-infrared portions of the spectrum," Limnol. Oceanogr. **38**(1), 188–192 (1993).
14. L. Trabjerg and N. K. Højerslev, "Temperature influence on light absorption by fresh water and seawater in the visible and near-infrared spectrum," Appl. Opt. **35**(15), 2653–2658 (1996).

#220552 - $15.00 USD Received 19 Aug 2014; revised 24 Sep 2014; accepted 24 Sep 2014; published 7 Oct 2014

15. H. Buiteveld, J. M. H. Hakvoort, and M. Donze, "The optical properties of pure water," Proc. SPIE **2258**, 174–183 (1994).
16. V. S. Langford, A. J. McKinley, and T. I. Quickenden, "Temperature dependence of the visible-near-infrared absorption spectrum of liquid water," J. Phys. Chem. A **105**(39), 8916–8921 (2001).
17. B. I. Lange, T. Brendel, and G. Hüttmann, "Temperature dependence of light absorption in water at holmium and thulium laser wavelengths," Appl. Opt. **41**(27), 5797–5803 (2002).
18. L. Kou, D. Labrie, and P. Chylek, "Refractive indices of water and ice in the 0.65- to 2.5-µm spectral range," Appl. Opt. **32**(19), 3531–3540 (1993).
19. P. Larouche, J. J. Max, and C. Chapados, "Isotope effects in liquid water by infrared spectroscopy. II. Factor analysis of the temperature effect on H2O and D2O," J. Chem. Phys. **129**(6), 064503 (2008).
20. J. B. Cumming, "Temperature dependence of light absorption by water," Nucl. Instrum. Methods Phys. Res. A **713**, 1–4 (2013).
21. J. J. Max and C. Chapados, "IR spectroscopy of aqueous alkali halide solutions: pure salt-solvated water spectra and hydration number," J. Chem. Phys. **115**(6), 2664–2675 (2001).
22. J. J. Max and C. Chapados, "Isotope effects in liquid water by infrared spectroscopy. III. H2O and D2O spectra from 6000 to 0 $cm^{-1.}$," J. Chem. Phys. **131**(18), 184505 (2009).
23. R. M. Pope and E. S. Fry, "Absorption spectrum (380-700 nm) of pure water. II. Integrating cavity measurements," Appl. Opt. **36**(33), 8710–8723 (1997).
24. D. M. Wieliczka, S. Weng, and M. R. Querry, "Wedge shaped cell for highly absorbent liquids: infrared optical constants of water," Appl. Opt. **28**(9), 1714–1719 (1989).
25. R. Röttgers, C. Häse, and R. Doerffer, "Determination of the particulate absorption of microalgae using a point-source integrating-cavity absorption meter: verification with a photometric technique, improvements for pigment bleaching, and correction for chlorophyll fluorescence," Limnol. Oceanogr. Methods **5**, 1–12 (2007).
26. J. Lyman and R. H. Fleming, "Composition of seawater," J. Mar. Res. **3**, 134–146 (1940).
27. Y. Maréchal, "Infrared spectra of water. I. Effect of temperature and of H/D isotopic dilution," J. Chem. Phys. **95**(8), 5565 (1991).
28. X. Quan and E. S. Fry, "Empirical equation for the index of refraction of seawater," Appl. Opt. **34**(18), 3477–3480 (1995).
29. R. W. Austin and G. Halikas, "The index of refraction of seawater," SIO Ref. No. 76–1, Scripps Inst. Oceanogr., La Jolla, 121 pp. (1976).
30. D. J. Segelstein, "The complex refractive index of water," Thesis (M.S.), Department of Physics, University of Missouri, Kansas City (1981).
31. J. J. Max and C. Chapados, "Infrared transmission equations in a five media system: gas and liquid," J. Math. Chem. **47**(2), 590–625 (2010).
32. M. Jonasz and G. Fournier, *Light Scattering by Particles in Water: Theoretical and Experimental Foundations* (Academic, 2007).

1. Introduction

The optical properties of pure water (H_2O) in both, liquid and gaseous, states are fundamental for the physical modelling of the atmosphere and ocean and for many optical remote sensing applications. The spectral features of light absorption by water in the visible to infrared spectral region are related to the fundamental rotational and vibrational modes of the water molecule, whereas electronic absorption plays a role only at shorter wavelengths. The dominant vibrational features of the two O-H bonds leading to major absorption maxima are symmetric (ν_1) and asymmetric (ν_3) stretching, and bending (ν_2) of the molecule with wavenumbers (wavelength) of approximately 3657 cm^{-1} (2734 nm), 3756 cm^{-1} (2662 nm), and 1595 cm^{-1} (6271 nm) in the gaseous phase of $H_2{}^{16}O$, respectively [1,2]. In the gaseous phase, rotation of the molecule is free and this leads to many rotational-vibrational combinations and millions of absorption lines. In the liquid state these rotations are limited by hydrogen bonding in the water molecule cluster and are reduced to three so-called libration modes that have weaker influences than the vibrations and are, hence, at lower wavenumbers. It also leads to a strong broadening of the major absorption lines; the absorption spectrum in liquid water is a continuum. Wavenumbers for the fundamental vibrations of liquid ordinary water at 25 °C are 3277 cm^{-1} (ν_1; 3050 nm), 3490 cm^{-1} (ν_3; 2870 nm), and 1645 cm^{-1} (ν_2; 6080 nm) [2,3]. Spectral absorption features in liquid water at wavelengths outside of these fundamental vibrations and librations are due to combination and harmonics of these fundamental vibration and libration modes. As temperature and ions dissolved in water change the internal structure of the water molecule cluster, the frequencies of these fundamental modes change and the light absorption spectrum of "pure" water changes with

#220552 - $15.00 USD Received 19 Aug 2014; revised 24 Sep 2014; accepted 24 Sep 2014; published 7 Oct 2014

temperature and the concentration of ions dissolved in it in a complex manner. Although absorption by ions in this spectral region is typically insignificant, changes in temperature and ion concentration do change the number of water molecules per volume by changing the density and partial density, respectively, thereby changing the absorption coefficient of water as well.

In optical oceanography the light absorption and scattering properties of liquid water need to be known and have been considered in many studies over the past years (for a review about absorption see [4]). As the quality of our spectral absorption measurements improves, knowledge of changes in these optical properties with temperature and seawater salinity requires better definition and resolution. Pure water optical properties contribute significantly to total inherent optical properties, particularly in clear oligotrophic waters, but also in particular spectral regions even in turbid coastal waters. Most of the *in situ* or lab-based measurements of the optical properties of water constituents (besides water) use pure water as the reference to facilitate spectrophotometric determination. These techniques generally do not require exact knowledge of the pure water properties. Nevertheless, temperature- and salinity-related differences have to be taken into account when the measured signal is in the same range as the differences induced by variations in temperature and salinity. This is certainly the case in most oceanic waters, but is also often true in more turbid coastal or inland waters. Therefore, the temperature and salinity correction coefficients for water absorption, Ψ_T and Ψ_S, respectively, have to be known. Ψ_T and Ψ_S are defined here by the absolute change in water absorption coefficient at wavelength λ, ($da(\lambda)$), with the change in temperature (dT) and salinity (dS), i.e. $da(\lambda)/d$T and $da(\lambda)/d$S, with units of [m^{-1} $°C^{-1}$] and [m^{-1} S^{-1}], respectively. The correction coefficient can be used to calculate differences in the water absorption coefficient for a known difference in temperature and salinity. Temperature difference can be reduced in laboratory measurements by adjusting the temperature of sample and reference before and during the measurement, but this is often not possible with in situ measurements, nor can difference in salinity between seawater and a pure water reference be avoided. These correction coefficients have been established, e.g. for specific in situ instrumentation [5–7]. The focus in oceanographic optics is on the visible (VIS) to near infrared (NIR) spectral range (300 – 800 nm), and to date Ψ_T and Ψ_S have mainly been given for this range only.

Temperature and salinity also change scattering by water. Light scattering by pure water, seawater, and some salt solutions can now be modelled with good accuracy for different temperature and salinity for, in principle, all wavelengths [8–11]. However, compared to absorption, scattering by water and seawater is negligible in the infrared spectral region. Effects of temperature on water absorption were shown by Collins (1925) for infrared wavelengths [12]. The temperature correction coefficient, Ψ_T, is now known from ~400 to 900 nm [5,6,13–16] and at single wavelengths in the infrared [17]. Data from determination of the water absorption coefficient performed at different temperatures and at IR wavelengths can be used to estimate Ψ_T [18,19] (Fig. 1). Additionally, attempts were made to model Ψ_T from the pure water absorption spectrum to estimate Ψ_T for wavelengths for which no data were available yet [5, 20].

Ψ_S was estimated for 400 to 800 nm from measurements of NaCl solutions [5,6] and can be determined from absorption coefficient measurements of pure salt solutions in the IR [21,22] (Fig. 2). No data for Ψ_S are available for the spectral region of 900 to 1600 nm, and FTIR data in the range of 1600 to 3000 nm are of lower quality. Therefore Ψ_T and Ψ_S were measured between 400 and 2500 nm with a spectrophotometer and a point-source integrating-cavity absorption meter (PSICAM), the latter providing path lengths of up to several meters in the VIS. The results can be combined with calculations of the coefficient made from FTIR measurement results of Max et al. (2001) [21] and Larouche et al. (2008) [19] to provide spectral distributions of Ψ_T and Ψ_S for the range of 400 to 14000 nm, and can be used to

#220552 - $15.00 USD Received 19 Aug 2014; revised 24 Sep 2014; accepted 24 Sep 2014; published 7 Oct 2014

correct optical measurement in liquid water and for modelling of optical properties of water in the VIS to IR region.

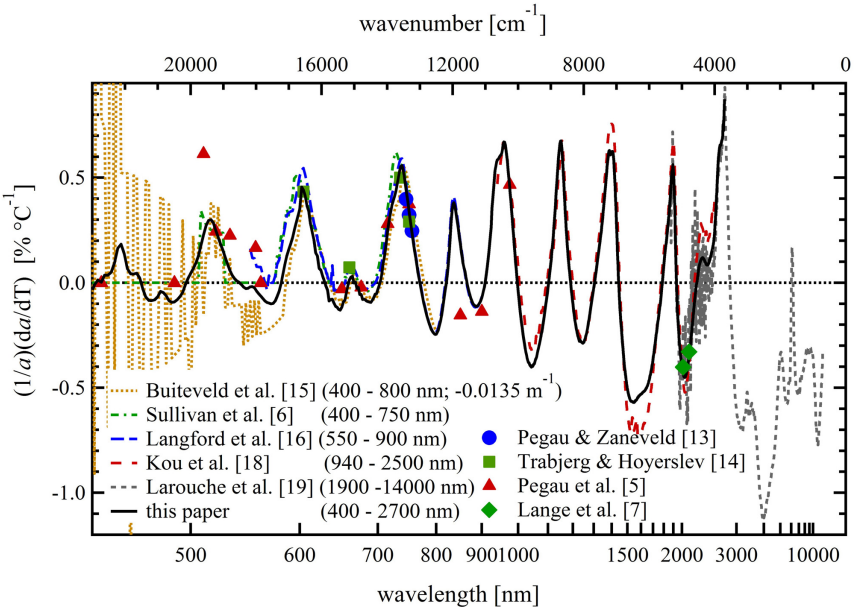

Fig. 1. Temperature correction coefficient for pure water light absorption, Ψ_T, as a function of wavelength and wavenumber. To depict a complete spectrum, Ψ_T is shown relative to the pure water absorption coefficient, a [m^{-1}], in $(1/a)(da/dT)$[% $°C^{-1}$]. Note: 1) the water absorption coefficient values were combined from published data at 400 – 700 nm [23], 660 – 2500 nm [18], and 850 – 15000 nm [24]; 2) data of Buiteveld et al. 1994 [15] are offset corrected by –0.0135 m^{-1}; 3) for Kou et al. 1993 [18]: Ψ_T was calculated from the difference in measurements of a for supercooled, liquid water at –8°C and liquid water at 22°C; 4) for Larouche et al. 2008 [19]: Ψ_T was calculated from the measurements of a for liquid water between 31°C and 61°C.

2. Methods

All spectrophotometric measurements were conducted in a Lambda 950 UV/VIS/NIR spectrophotometer (Perkin Elmer) using cuvettes with path lengths between 0.1 and 100 mm. Additional measurements were performed with a point-source integrating-cavity absorption meter (PSICAM) in the spectral range of 400 – 800 nm, which for low pure water absorption coefficients has a theoretical path length of up to three meters and, hence, provided more precise measurements at < 700 nm.

The spectrophotometer was regularly calibrated for wavelength accuracy and intensity. Its non-linearity error was determined several times with a double aperture setup and was always close to the manufacturer's specification. With each setup and type of cuvette the alignment of the beams was controlled and if necessary adjusted, e.g. the height of the beam was adjusted by software settings to fit to the individual cuvette window sizes. Slit width was 2 nm for the spectral range of 400 to 860 nm. At longer wavelengths, where transmission through the cuvette was low, the slit width was automatically adjusted to obtain a good sensitivity, in optimum case (shortest path length) this was < 2 nm, but occasionally up to 20 nm in the vicinity of the strong absorption features of water at ~1900 and > 2500 nm. Due to the strong changes in water absorption with wavelength over this spectral range, a cuvette of a specific path length can only be used for a narrow wavelength range (see Table 1). Data were collected with the use of these different path length cuvettes in several scans, in total between 400 and 2700 nm in 1 nm intervals. Scan speed was adjusted (between 0.3 and 2 s per nm) for

#220552 - $15.00 USD Received 19 Aug 2014; revised 24 Sep 2014; accepted 24 Sep 2014; published 7 Oct 2014

different wavelength regions to get good signal to noise ratios. The instrument was turned on 1 hour before the first measurement, the baseline was recorded with reference and sample cuvette filled with purified water at room temperature or at a specific temperature using a thermostatic water bath and temperature controllable cuvettes (see below).

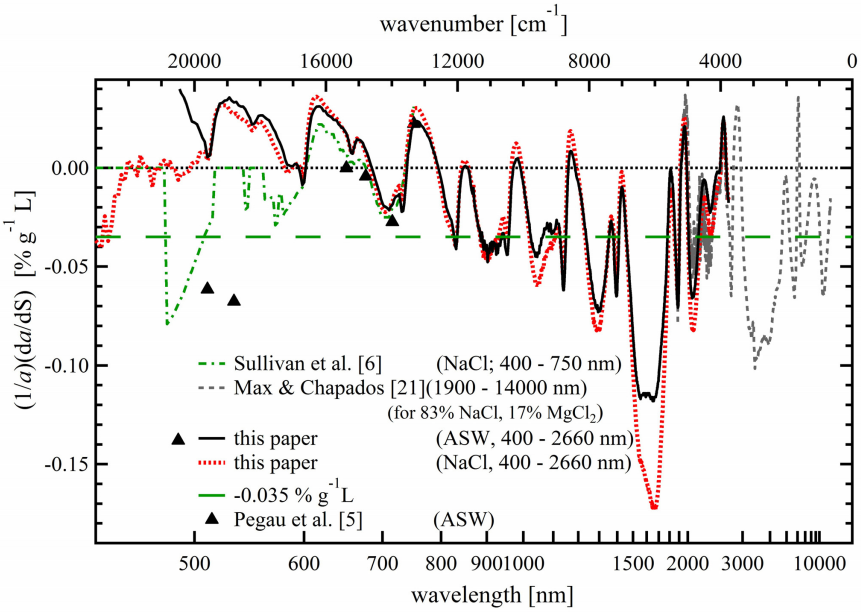

Fig. 2. Salinity correction coefficient for pure water light absorption, Ψ_S, as a function of wavelength and wavenumber. To depict a complete spectrum, Ψ_S is shown relative to the pure water absorption coefficient, a [m^{-1}], in $(1/a)(da/dS)$ [% $(g\ L^{-1})^{-1}$], where salinity is expressed as salt concentration in g L^{-1}. Note: The water absorption coefficient values were taken from published data at 400 – 700 nm [23], 660 – 2500 nm [18], and 850 – 15000 nm [24]. The type of salt used to determine Ψ_S is indicated; ASW is artificial seawater. For Max and Chapados 2001 [21], Ψ_S was calculated from measurements of a for salt solutions of NaCl and $MgCl_2$ with the concentration ratio of these salts in seawater as indicated. A dashed line indicates a –0.035% (g L^{-1}) reduction of the water absorption coefficient due to a decrease in number of water molecules per volume.

PSICAM measurements were performed as described elsewhere [7,25]. An Avantes ULS2048XL detector with a 100 µm slit (optical resolution: ~3 nm) and a CF-1000 (Illumination Technology) light source were used. The instrument was calibrated against the spectrophotometer using colored solutions of Nigrosine by measuring the solutions with a 10 cm cuvette in the spectrophotometer against purified water to determine its absolute absorption coefficient, and subsequently measuring it with the PSICAM.

Purified water was taken from a water purification system (Millipore), consisting of an Elix system, a water tank for deionized water with UV treatment, and finally a Gradient system, providing 0.2 µm filtered water at > 18.2 MOhm cm^{-1} resistivity and < 3 ppm total organic carbon. The water was filled in acid cleaned glass bottles and left in the lab for only a few hours to gain room temperature. Longer storage was avoided as build-up of particles could often be observed that would increase scatter losses. The water used is considered to be free of organic contaminants and of particles > 0.2 µm.

2.1 Salinity correction coefficients

Determination of the salinity coefficient was performed using a concentrated NaCl (> 99.5% pure, Merck) solution as an equivalent for seawater, and a concentrated artificial sea water (ASW) solution prepared from different salts with the same composition as the major salts of

#220552 - $15.00 USD Received 19 Aug 2014; revised 24 Sep 2014; accepted 24 Sep 2014; published 7 Oct 2014

natural sea water (sea water salt components with less than 1% contribution were not included for simplicity). NaCl salt of higher purity (> 99.99%, optical grade, Sigma) was tested, but did not show lower contamination by impurities visible as strong absorption in the ultraviolet.

Table 1. Spectral measurement ranges for cuvettes of different path length.

path length (mm)	wavelengths (nm) for Ψ_S	wavelengths (nm) for Ψ_T
100	400 - 1000	400 - 1000
10	860 - 1350	900 - 1350
5	900 - 1800	950 - 1850
2	1250 - 2250	1300 - 2300
1	1350 - 2350	1350 - 2400
0.2	1750 - 2660	1350 - 2660
0.1	not used	1350 - 2660

It has been shown previously that the change in water absorption with salt concentration at one wavelength is linear [5,6], so only one concentrated solution was used in each case, no measurements were done with dilute solutions. The NaCl solution was prepared by diluting 71.9 g of combusted (500°C for 4 h) NaCl in purified water to a final volume of 1.00 L, yielding a concentration of 71.9 g L^{-1} or 68.4 g kg^{-1}. This concentration was used to make results comparable to the ASW measurements, as here for some of the salts the maximum solubility is reached with concentrations of total salts > 72.0 g L^{-1}. The ASW [26] was prepared by dissolving combusted quantities (500°C for 4 h) of NaCl (49.96 g), KCl (1.33 g), KBr (0.19 g) and non-combusted quantities of $MgCl_2{\cdot}6H2O$ (21.24 g), Na_2SO_4 (7.84 g), $CaCl_2{\cdot}2H2O$ (3.04 g) and $NaHCO_3$ (0.38 g) in purified water to a final volume of 1.00 L. The final salt concentration was 71.9 g L^{-1}, the density was 1049 g L^{-1}, and the mass concentration was 68.5 g kg^{-1}.

To remove particles that would either absorb or scatter light, the solution was first vacuum filtered through 0.2 µm using acid-cleaned glassware and membrane filters (GWSP; Millipore). Three times 100 mL were filtered and discarded to wash and rinse the filter and the glass ware. The remaining 700 mL were filtered, filled into a clean glass bottle. As it was observed that vacuum filtration increased the scattering signal of the solution, probably by a build-up of small bubbles during vacuum filtration, in a second step the solution was filtrated by pressing it with the help of a 50 mL clear plastic syringe through a 30-mm syringe filter (Spartan A27, 0.22 µm pore size). The syringe and the filter were rinsed before with 400 mL purified water and with 50 mL of the solution. After this rinsing no additional contamination of the solution was observed in UV absorption measurements. After the first filtration the used filter showed a visible dark color, indicative for absorbing particles in the prepared solution. As particles smaller than 200 nm cannot be filtered out with this procedure and other absorbing contaminations are expected, the usually high absorption of ultraviolet radiation did not allow to measure the salinity coefficient at wavelengths < 400 nm, especially with the artificial seawater, where UV-absorption by some of the salts (e.g. bromide) was expected and observed.

In the spectrophotometer the solutions were measured against a purified water reference in regular glass cuvettes (Hellma Analytics; type 100-QS) and in temperature controllable cuvettes (Hellma Analytics; type 165-QS) at 20.0°C, no significant difference were observed as measurements are typically performed at a room temperature of 20°C. These cuvettes were not removed from the sample compartment of the spectrophotometer between replicate measurements, and instead the sample volume in the cuvette was exchanged using a pipette. This avoided moving the cuvette and thereby reduced offset artefacts due to small reflection changes in the air to glass interface. The sample was exchanged three times to rinse the cuvette before the measurement was started. For different spectral regions, cuvettes with

#220552 - $15.00 USD Received 19 Aug 2014; revised 24 Sep 2014; accepted 24 Sep 2014; published 7 Oct 2014

different path lengths were used (Table 1) to compensate for the absolute transmission through the cuvette at different wavelengths due to the strongly increasing absorption by water with increasing wavelength. For most wavelengths several path lengths could be used and several OD-spectra were obtained. For the NIR region, these overlapping spectra also differ in the automatically adjusted slit width and, hence, spectral resolution. However, in the final analysis the results with the best signal to noise ratio were selected. The shortest path length used was 0.2 mm as data collected with even shorter path length showed signs of an interference pattern forming in the OD spectrum.

With the PSICAM the solutions were measured ten times against purified water at the same temperature. Temperature could not be controlled and was, hence, measured shortly before each light measurement. Small temperature differences (< 0.2°C) between a solution and the reference were corrected using the later obtained temperature correction coefficient (see below).

2.2 Temperature correction coefficients

Spectrophotometric measurements of the temperature coefficient were performed in temperature-controllable cuvettes (Hellma Analytics; type 165-QS). The cuvettes' (sample and reference) outer flow-through jacket was connected with plastic tubes to two water baths (DC1 and DC 50; both from Haake): one bath was set to 15°C and the other to 60°C. By using two three-way valves both water baths could be connected independently to both jackets, to facilitate a fast change of the temperature inside the cuvettes. The time needed for the temperature inside the cuvette to stabilize after a change and the absolute temperature in both cuvettes had been determined before each spectrophotometric scan and with each set of cuvettes with an electronic thermometer equipped with a small PT-100 probe (precision ± 0.1°C) that fitted inside all cuvettes. The electronic thermometer was calibrated before against a mercury-thermometer with an accuracy of ± 0.05°C. The baseline was collected when reference and sample cuvette were filled with purified water and kept at the same temperature of 15.0°C. Afterwards the temperature in the sample cuvette was changed to 60.0°C as described above. After the necessary time for stabilizing the temperature had passed, the OD scan was started. As with the salinity coefficient, it has previously been shown that the light absorption at a specific wavelength changes linearly with temperature [6,12] (but see [27]), hence, the difference in temperature between baseline and sample measurements was used to determine the temperature coefficient of the absorption. Lower and higher temperatures were not used to avoid water condensation on the cuvette windows and weakening of the plastic tubes, respectively. This measurement procedure was done with cuvettes of different path lengths for different wavelength regions (Table 1).

With the PSICAM the absorption coefficient difference between two purified water samples of temperatures between 15°C and 55°C was determined ten times. One purified water sample was heated in a water bath and another cooled in a refrigerator. The actual temperature of each sample was measured shortly before the light intensity measurement. This process resulted in recording of ten absorption difference spectra and corresponding temperature differences.

2.3 Corrections

Changing the temperature and/or ion concentration in water also changes the real part of the refractive index of water and scattering by water/solution. For the spectrophotometric measurements, the refractive index of the cuvettes' glass material, the glass window thicknesses, and the path length also change with temperature. The changes in glass refractive index, window thickness, and path length with temperature were negligible compared to the general measurement error, the latter induced by variations in scattering from small particles (micro bubbles) and small changes in the optical path when the cuvettes were manipulated. Changes in reflectance/transmittance due to changes in refractive index with the salt

#220552 - $15.00 USD Received 19 Aug 2014; revised 24 Sep 2014; accepted 24 Sep 2014; published 7 Oct 2014

concentration were significant, and led to a negative offset with only a very small wavelength-dependence and needed to be corrected. The reflectance and transmittance changes over the different cuvette window surfaces (air to glass, glass to water, etc.) were calculated using Fresnel's equations for a perpendicular light beam and the measured OD was corrected for these changes. Therefore the refractive index of the respective cuvette glass (Suprasil®) as well as the coefficient of change of this index with temperature was taken from manufacturers' information (Heraeus Quarzglas). The refractive index of water for different temperatures and salinities was calculated for each temperature and salinity using equations provided by Quan and Fry (1995) [28] which are based on data of Austin and Halikas (1976) [29]. Data were available for the range of 400 – 800 nm only and extrapolated to longer wavelengths using the spectral distribution of the refractive index as provided by Segelstein (1981) [30]. From the corrected OD the absorption coefficient was calculated by a (m^{-1}) = ln(10) * OD / L, where L is the path length in meter, when OD = -log(T), with T is the transmittance.

In addition the scattering coefficient of water for different temperatures and that of the NaCl solution was calculated after Zhang et al. (2009) [10,11], and subtracted from the calculated absorption coefficient. The influence of this difference in scattering was only visible at the shortest wavelengths (< 600 nm).

Artificial negative offsets were visible after these corrections that, however, were often smaller than the actual measurement errors (determined from repetitions) and are assumed to be due to multiple reflections at the cuvette windows that were not considered here and small changes in the optical path by small differences in the positioning of the sample and reference cuvette when the cuvettes had to be changed to use different path lengths. Both effects are considered to be wavelength-independent, and the wavelength-independence was actually seen in small differences of repetitive measurements. This offset was corrected manually assuming that the determined T and S coefficient is close to zero at wavelengths of very low water absorption, i.e. at ~420 nm, and that this offset is wavelength-independent. This can be done only for the spectra that included 420 nm. The concomitant spectra starting at longer wavelengths were adjusted accordingly to give the same values as the already corrected spectra in the overlapping spectral region. By these adjustments a complete spectrum was constructed.

Finally the data from different spectra (obtained with different path lengths) were combined by taking the mean of all spectra available for one wavelength, when all spectra had been measured with an appropriate optical resolution (according to the automatically adjusted slit width at > 860 nm) of < 4 nm and a good signal to noise ratio. At spectral regions of strong water absorption, when optical resolution and the signal to noise ratio was lower, the data of the spectrum with the best optical resolution was used, this was always obtained with the shortest path length. The best optical resolution in these spectral regions could also be ascertained by noticeably stronger spectral features that are attenuated by a lower optical resolution. In the spectral region of strong water absorption the results are taken from just one spectrum with the shortest path length, at other wavelengths they represent the average of measurements performed with three different path lengths, which were consistent except for the issues due to differences in optical resolution.

Verification of these adjustments was done using an optical model for cuvette measurements. This model is based on the calculation scheme of Max and Chapados (2010) [31] providing analytical equations for the determination of light transmission through a cuvette (i.e. a sample between two glass windows) using known optical properties. These properties are the complex refractive index of the glass material and that of water, including changes induced by temperature and salinity, and scattering of water and its changes with temperature and salinity. The final temperature and salinity coefficient for water absorption were used. The information of the refractive indices for glass were the same as described above. Water absorption is taken from Pope and Fry (1997) [21], Kou et al. (1989) [18],

#220552 - $15.00 USD Received 19 Aug 2014; revised 24 Sep 2014; accepted 24 Sep 2014; published 7 Oct 2014

Wieliczka et al. (1989) [22], and Max and Chapados (2009, for 1850-2000 nm and > 2500 nm) [22]. In addition the scattering of a NaCl solution (in g kg^{-1}) at 589 nm was determined after Zhang et al. (2009) [11]. As proposed by Zhang et al. (2009) [11] the full scattering spectrum is obtained by using spectral results from calculations after Zhang et al. (2009) [10] for an equivalent salinity that is adjusted by shifting the whole spectrum, so that the values at 589 are the same. The transmission model calculates the OD for a specific cuvette at a specific temperature, with known properties (of glass material, window thickness, and path length) that is filled with water at a specific temperature and with a specific NaCl concentration. Differences in OD with temperature and salt concentrations were calculated and compared with the original measurements that represent the difference of a sample to a specific reference.

For the PSICAM, temperature and salinity will change the reflectance/transmittance at all optical relevant surfaces, i.e. at the inner wall of the cavity, at the quartz-glass surface of the central light source (changing the light throughput from the lamp), and at the tip of the optical fiber towards the detector, as well changing the field of view of the detector. Due to the PSICAM's design, any change in scattering can be ignored. The sample temperature might additionally change the whole optical setup, by changing the temperature of the different mechanical components. However, the highly reflective bulk material is a good insulator, so temperature differences will only occur close to its inner surface. On the other hand it is a lambertian reflector, where reflection is the result of strong scattering inside the material, not at the surface, significantly reducing the influence of refractive index changes at the transmission surface. Therefore the strongest influences are expected at the quartz-glass surfaces of the central light source and the fiber optics. Effects of the changes in refractive index by temperature difference are expected to be negligible, but those due to salt concentration might be significant. The potential changes are considered to be mainly wavelength-independent. The absorption difference at wavelengths at which no or very low changes are expected (400 – 420 nm) can give evidence for the extent of such changes. For the temperature effect the absorption coefficient difference at 400 nm are close to zero, for the salt concentration effect the signal at 400 – 500 nm was slightly negative in the case of NaCl (for ASW it was higher due to contamination problems). However, the absolute values were below the typical precision of the PSICAM (< 0.0008 m^{-1}). The optical setup of the PSICAM cannot be modelled in a simple way as is done for the cuvette setup and no validation of the effects can be performed.

For the resulting temperature correction coefficient, the PSICAM and spectrophotometric results were very similar in the spectral range of 600 – 700 nm and only a small offset correction (+ 0.000023 m^{-1} $°C^{-1}$) was applied to the PSICAM results to give a zero value at 420 nm. In case of the salinity correction coefficient the PSICAM results showed the same spectral structure as the spectrophotometer, but absolute values deviated clearly from the spectrophotometric results (see below). The deviations were wavelength-dependent on the absolute coefficient scale (m^{-1} $g^{-1}L$) and followed the water absorption spectrum, hence, were rather wavelength-independent on the relative difference scale (% $g^{-1}L$). Here a positive offset of 0.015% $g^{-1}L$ is observed and was consequently subtracted as spectrophotometric measurements are assumed here to give the correct results. The reason for this difference to the spectrophotometric determination is probably that reflectance changes at the inner wall surface of the PSICAM with changes in the real part of the refractive index (water vs. salt solution) could not be corrected.

2.4 Additional data

Additionally Ψ_T for the near infrared region (1870 – 14280 nm) was determined from measurements of water absorption at different temperatures [19], the spectral data were

#220552 - $15.00 USD Received 19 Aug 2014; revised 24 Sep 2014; accepted 24 Sep 2014; published 7 Oct 2014

provided by J.-J. Max (pers. comm.). Ψ_T and its standard error were determined from linear regression analysis of measurements at 31.3, 40.6, 50.0, and 60.5°C.

Ψ_S for the near infrared region (1890 – 15000 nm) was calculated from absorption data of water and concentrated NaCl and $MgCl_2$ solution [21], these were the salts of seawater for which data are available. The spectral data were provided by J.-J. Max (pers. comm.). From the difference in absorption of water and the solution, and the salt concentration of the solution, a spectrum for Ψ_{NaCl} and Ψ_{MgCl2} was calculated for pure NaCl and $MgCl_2$, respectively. To estimate Ψ_S for seawater the final value was calculated according the typical mass concentration of $MgCl_2$ in seawater (~17%) [26], and replacing all other salts with NaCl (~83%) as $\Psi_S = 0.17\Psi_{MgCl2} + 0.83\Psi_{NaCl}$.

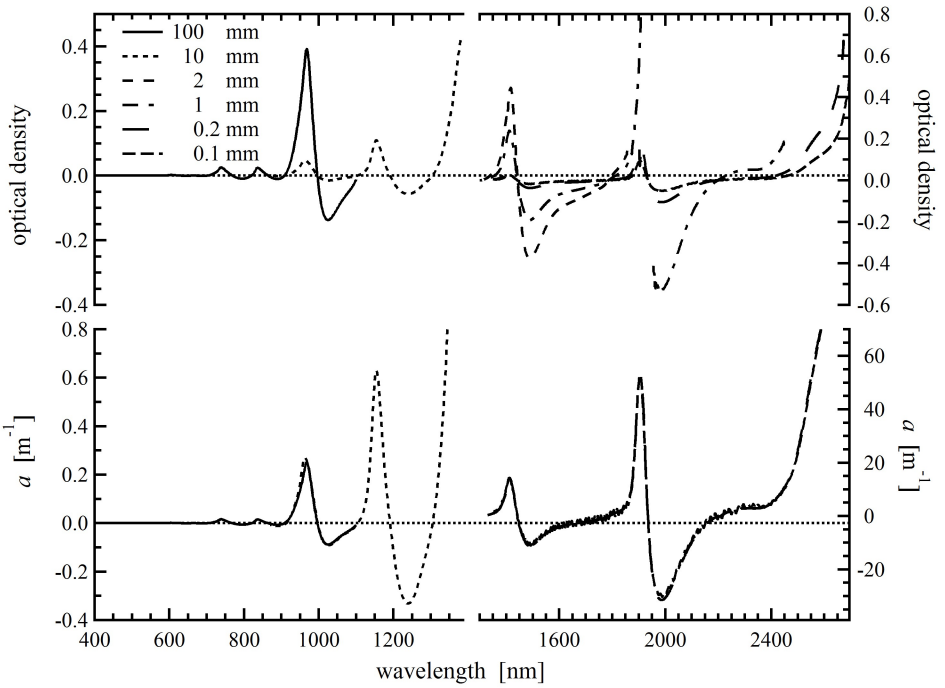

Fig. 3. Difference spectra of optical density (upper panels) and the corresponding difference in absorption coefficient (*a*) (lower panels) for pure water of 15° vs. 60°C. Measurements are performed with cuvettes of different path length as indicated in the legend and for different wavelength ranges with each cuvette (see Table 1).

3. Results and discussion

3.1 Temperature correction coefficient

The optical density (OD) difference spectrum (15° vs. 60°C) of pure water measured with cuvettes of difference path lengths (Fig. 3) in the spectrophotometer shows very small deviations from zero at the shortest wavelengths (< 500 nm). This demonstrates that influences by changes in refractive index (real part) and scattering with the temperature were relatively small. After correction of these marginal effects and calculating the difference in absorption coefficients, *a* (in m^{-1}), spectra obtained for different path lengths agreed very well. Deviations at some pronounced spectral features in the NIR (e.g. at ~960 nm in Fig. 3, lower panels) were caused by differences in the optical resolution (i.e. differences in the slit width used). For the final spectrum these spectra are combined and in regions of the pronounced spectral features the data from the respective spectrum that was measured with the shortest path length, i.e. with the best optical resolution, is used. The spectrum measured with a path length of 0.1 mm was not used due to the strong inference pattern in the whole

#220552 - $15.00 USD Received 19 Aug 2014; revised 24 Sep 2014; accepted 24 Sep 2014; published 7 Oct 2014

spectrum (Fig. 3, lower right panel), and because data with the 0.2 mm cuvette were available.

PSICAM measurements of Ψ_T for 400 to 700 nm (Fig. 4) agreed well with the spectrophotometric results, but provided much better precision. Here a maximum at ~516 nm and a shoulder at ~550 nm are clearly visible. Note that both spectra in Fig. 4 are offset corrected (by ~0.000023 m^{-1} $°C^{-1}$) to compensate for small wavelength-independent measurements artifacts, assuming zero values for Ψ_T at 420 nm, i.e. at the pure water absorption minimum [23].

In principal density changes with temperature do change the pure water absorption coefficient. When density decreases the number of molecules per volume or optical path decreases. For pure water, density changes with temperature are not linear, maximum density is reached at 4°C and increases with decreasing and increasing temperature. For the experiments here a change from 15°C to 60°C changes the density of pure water by −1.6% from 0.9991 to 0.9832 kgL^{-1}, the number of water molecules per liter changes accordingly from 55.44 M to 54.56 M. Taking the density change as being linear would result in a relative change of the absorption coefficient by −0.036% per °C, a rather small bias compared to the values of Ψ_T shown in Fig. 1.

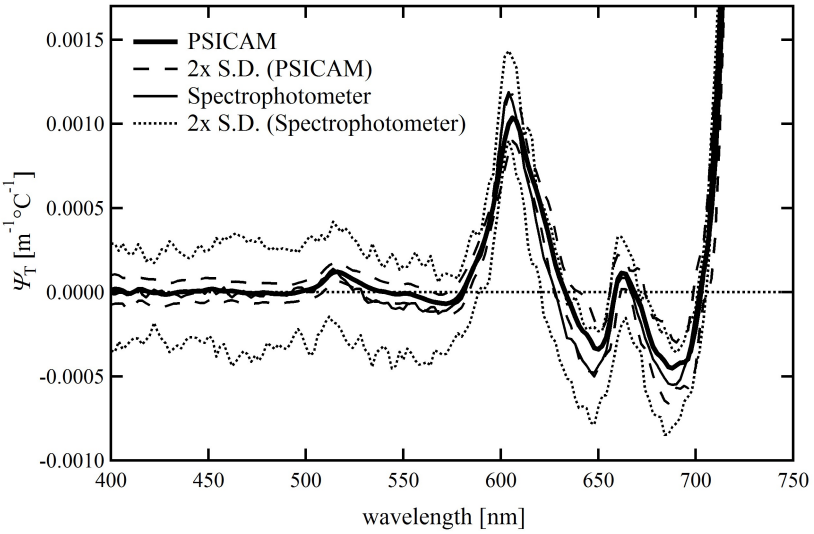

Fig. 4. Calculated temperature correction coefficient, Ψ_T, (± 2 S.D. vs. wavelength) for spectrophotometer measurements in a 100 mm cuvette, together with that obtained from PSICAM measurements.

The two resulting spectra of Ψ_T for spectrophotometer and PSICAM are combined by using PSICAM results for 400 - 700 nm and at 702 - 2660 nm the spectrophotometric results. This final spectrum of Ψ_T for the VIS to NIR region is shown in Fig. 5. Known spectral features in the VIS and short NIR (< 900 nm) are observed, with maxima at ~606, 662, 739, and 837 nm, a new small maximum is also visible at ~516 nm. Local minima are observed at 572, 648, 688, 798, and 890 nm. At longer wavelengths further spectral features are observed with maxima at ~966, 1154, 1412, and 1905 nm, and minima at ~1027, 1240, 1490, and 1986 nm. The strength of the maxima and minima increased with wavelength by five orders of magnitude over the spectral range of 600 to 2660 nm, proportionally with the increasing water absorption coefficient.

These measurements of Ψ_T reproduced earlier results for this spectral range [6,15–19] (Fig. 1). As expected, the spectrophotometric results for the spectral range of 1000 - 2600 nm are more precise and showed lower noise than the results of the FTIR measurements. At < 700 nm deviations between the different spectra are visible but are in the range of the

#220552 - $15.00 USD Received 19 Aug 2014; revised 24 Sep 2014; accepted 24 Sep 2014; published 7 Oct 2014

measurement errors of the earlier determinations. At > 700 nm, deviations stronger than explainable by measurement uncertainties are visible around the maxima at 740 nm and 1400 nm, and the minima at 1050 and 1600 nm. In this spectral range Ψ_T was calculated from pure water absorption coefficients at two different temperatures provided by Kou et al. (1993) [17] that included results of supercooled, liquid water at −8°C. Supercooled water might not be representative for liquid water in general. Besides these deviations the different determinations of Ψ_T do agree well but the new data have lower uncertainty levels, and showed reproducibility with independent measurements in the visible range by spectrophotometric and PSICAM measurements.

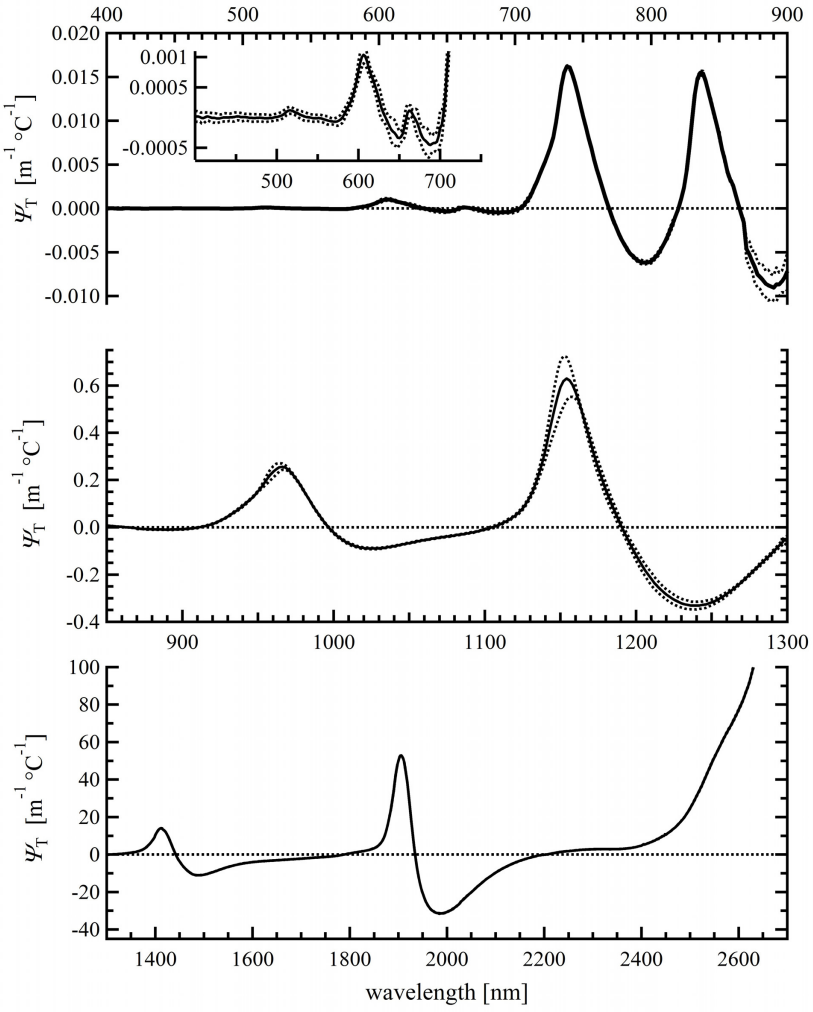

Fig. 5. Temperature correction coefficient for pure water, Ψ_T, in the spectral range of 400 - 2600 nm (Media 1). Given is the mean and 2xS.D. (n = 5 - 10). Note that in the lower panels the S.D. is smaller than the line thickness.

Previous studies have attempted to estimate Ψ_T using models [5,32]. A Gaussian fit procedure of the water absorption spectrum at 20°C was used and a temperature change of about 0.5% per °C applied to each of these Gaussians [5,32]. Each Gaussian represented the absorption overtone of either of two types of water molecule cluster sizes (single to several molecules vs. large number of molecules in clusters). The change in the absorption coefficient

#220552 - $15.00 USD Received 19 Aug 2014; revised 24 Sep 2014; accepted 24 Sep 2014; published 7 Oct 2014

by a temperature change was explained by a higher temperature increasing the number of small clusters and decreasing the number of larger clusters, as an increase in molecular movements with temperature increases the rate of breaking of the hydrogen bonds forming the clusters. Recently the use of the derivative of the absorption spectrum was suggested for modeling of Ψ_T, as a good correlation of the minima in the derivative spectrum and the maxima in Ψ_T was found [20].

Additional spectral features in Ψ_T could be reliably observed with a local maximum at ~516 nm and a shoulder at ~550 nm. The maximum at 516 nm is already indicated elsewhere [6,15], and was theoretically expected by the modeling [32, *see* 20]. From this modeling another maximum is expected at ~450 nm [*see* 20], and there is a suggestion of this in the data presented here (Fig. 1) but the extent of the maximum is still in the uncertainty range. Below 440 nm all features of Ψ_T are below the detection limit, and the coefficient is very close to zero as is expected since the pure water absorption coefficient is at its minimum [21] (note that Ψ_T was set to zero at 420 nm to correct for small remaining measurements artifacts induced by refractive index changes; see above).

These results can be combined with the data of Ψ_T calculated from FTIR measurements at 2600 – 14000 nm [19] (Fig. 1). A full Ψ_T spectrum was thereby constructed for 440 to 14000 nm [see Media 1]. Values for 300 to 440 nm were below the detection limit and, hence, can be assumed to be not significantly different from zero at the moment.

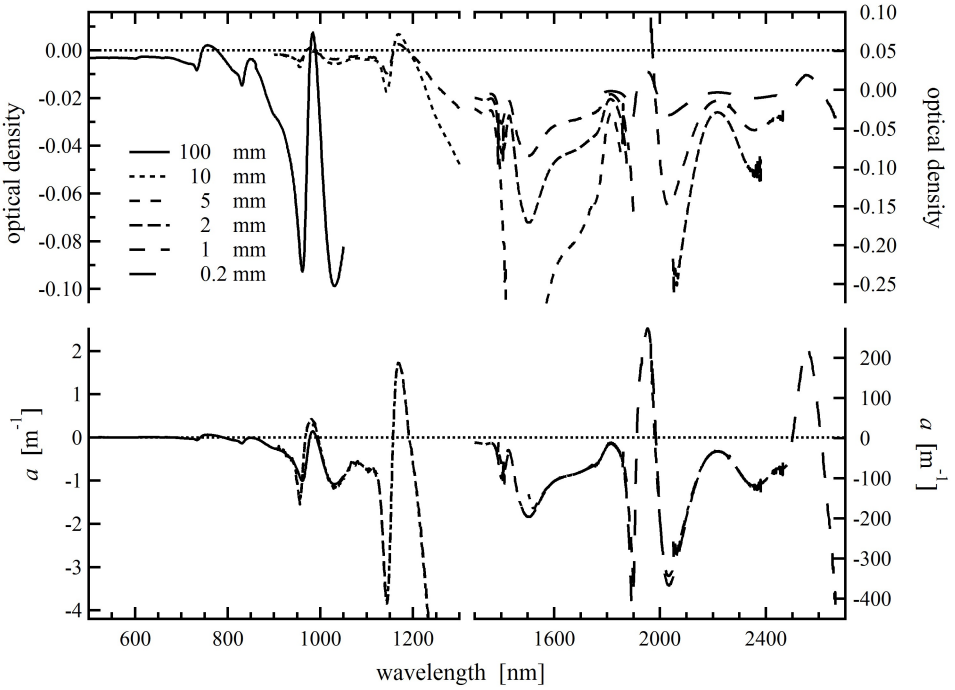

Fig. 6. Difference spectra of optical density (upper panels) and the corresponding difference in absorption coefficient (a) (lower panels) for NaCl solutions compared to pure water. Measurements are performed with cuvettes of different path length as indicated in the legend and for different wavelength ranges with each cuvette (see Table 1).

3.2 Salinity correction coefficient

Spectrophotometrically obtained OD difference spectra of the two salt solutions showed clear negative offsets at shorter wavelengths due to the difference in the real part of the refractive index of pure water and the concentrated salt solutions. These offsets were corrected as described above after differences in scattering had been subtracted. Outside this region the difference spectra showed clear maxima and minima (Fig. 6, upper panels). However, the

#220552 - $15.00 USD Received 19 Aug 2014; revised 24 Sep 2014; accepted 24 Sep 2014; published 7 Oct 2014

signal level was lower than during the temperature difference measurements, with absolute OD maximally 0.25. The spectral structure can, like for the above measurements of Ψ_T, be quite exactly reproduced by measurements with different path lengths, as can be seen in the calculated differences in *a* (Fig. 6, lower panels). Due to the generally lower OD, the stronger changes in scattering with salinity, and the higher offset correction needed, the relative measurements uncertainty for Ψ_S determination are generally larger than for Ψ_T.

PSICAM measurements with the NaCl solution showed similar spectral features as the spectrophotometric measurements at 400 – 750 nm range, but provided more precise data (Fig. 7). Clear deviations are visible between the PSICAM and the spectrophotometric determination, but when the above described correction for this absorption dependent offset was applied they agree well for both salt solutions (NaCl and ASW, for NaCl see Fig. 7). Due to the lower level of measurement uncertainties with the PSICAM and much lower noise in the spectra, the PSICAM results for Ψ_S are used for wavelengths < 740 nm, but due to applied correction they are not considered as being independent from the spectrophotometric measurements as in the case of the Ψ_T.

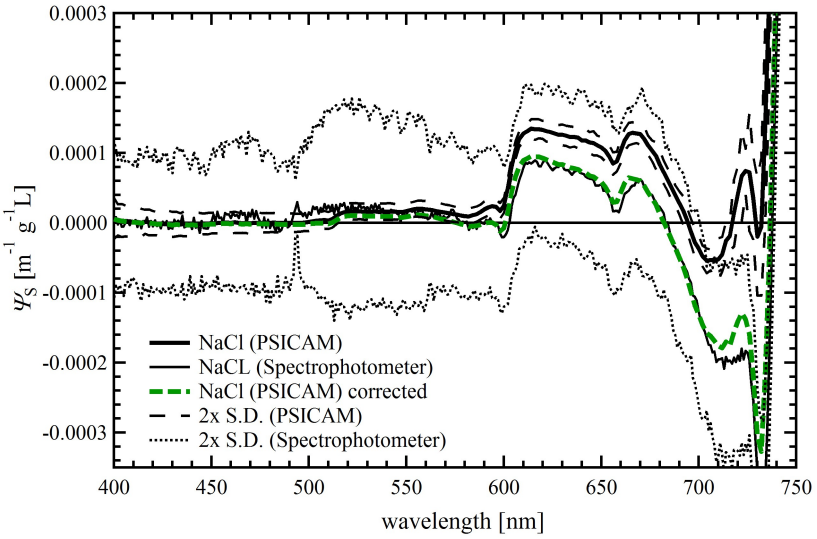

Fig. 7. Salinity correction coefficient, Ψ_S, (±2 S.D. vs. wavelength) calculated from measurements of a NaCl solution for spectrophotometer measurements in a 100 mm cuvette, together with that obtained from PSICAM measurements. Spectrophotometer results are offset-corrected at 420 nm; PSICAM results are not offset-corrected. Additionally shown in green is the spectrum of the PSICAM results corrected for a 0.015% g^{-1} L offset.

The PSICAM and all spectrophotometric results were combined. Here the spectrum measured with a path length of 0.2 mm had to be used despite the visible interference pattern, this pattern was removed by smoothing the spectrum. This smoothing did not significantly distort the spectrum in the overlapping region when comparing results for different path lengths. The final spectral results of Ψ_S determined for NaCl and ASW solutions are depicted in Fig. 8 together with the uncertainty in measurements for the NaCl solution (ASW uncertainties were similar). The two spectra show clear differences in Ψ_S at all wavelengths, the differences were generally greater than the range explained by uncertainties. In addition, there is a clear increase of measured Ψ_S at the shortest wavelengths for ASW that is not visible for the NaCl solution. This is considered to be a result of optical contamination occurring either during the salt solution preparation, which is more extensive than for NaCL, by contamination from one of the pure salts used, or simply by a real absorption of bromide in the ASW solution. This contamination makes determination of Ψ_s with ASW at wavelengths < 500 nm unreliable.

#220552 - $15.00 USD Received 19 Aug 2014; revised 24 Sep 2014; accepted 24 Sep 2014; published 7 Oct 2014

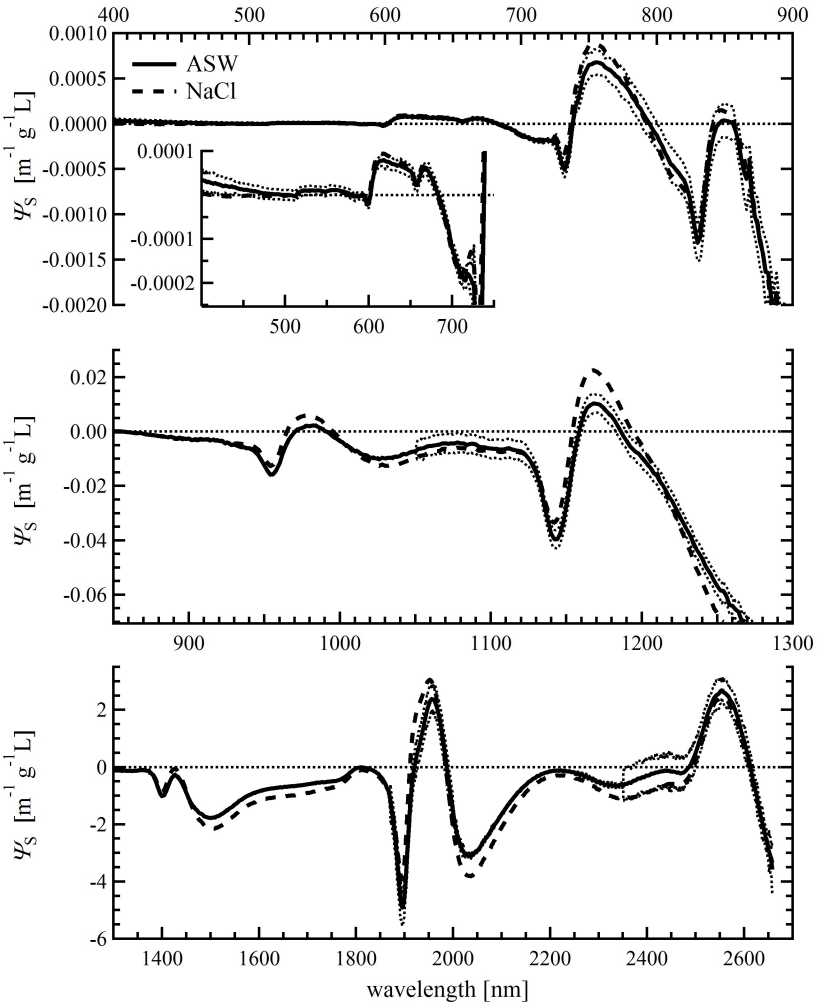

Fig. 8. Salinity correction coefficient for pure water, Ψ_S, in the spectral range of 400 - 2660 nm (Media 2). Given is the mean and 2xS.D. (n = 5 - 10) for artificial seawater (ASW). Additionally shown is the spectrum for NaCl without S.D. for clarity.

Nevertheless, it is suggested that the ASW spectrum is taken to represent Ψ_s for seawater at wavelength > 500 nm due to the visible deviations from the NaCl solution. Similar differences between NaCl and ASW were not observed in previous studies, likely due to the lower optical resolution of the instrumentation used [5,6]. These differences will still be small in the visible region, but get significant in the NIR. However, the typically observed trough in spectrophotometric measurements of seawater at 732 nm [7] is better represented by the ASW-derived Ψ_s spectrum, indicating that the ASW is closer to seawater than just a NaCl solution. The main reason for the difference between pure NaCL and ASW is the influence of different salts, especially $MgCl_2$, that contribute to the total salt concentration. Previous studies with pure salt solutions using Attenuated Total Reflection IR (ATR-IR) spectroscopy have shown that different alkali halide salts have different effects on the water absorption [21]. Most salts showed essentially similar spectral features but differed in the intensity of those features, but $MgCl_2$ showed spectral differences, i.e. clear shifts of the spectral features. The differences observed here are mainly attributable to a stronger intensity in the spectral features in Ψ_S with pure NaCl.

#220552 - $15.00 USD Received 19 Aug 2014; revised 24 Sep 2014; accepted 24 Sep 2014; published 7 Oct 2014

The final Ψ_s spectrum (Fig. 8) showed previously known spectral structures with a broad maximum at 610 to 680 nm, and one at 754 nm, and local minima at 659 nm and 732 nm. Another broad maximum is now apparent at 510 to 580 nm and a local minimum at 600 nm. Further in the NIR to SWIR region several distinct maxima are observed at 850, 982, 1170, 1427, 1956, and 2554 nm, and minima at 830, 955, 1142, 1403, and 1895 nm. Additionally, broader local minima and maxima are found throughout the spectrum. On a relative basis the values of Ψ_s varied between –0.18 and 0.04% g^{-1} L, with a clear trend towards more negative values with higher absolute pure water absorption coefficient values (Fig. 2). This can be explained by the fact that the ions replace water molecules in a fixed volume and do not contribute to light absorption, thereby reducing the number of water molecules per unit optical path, hence, decreasing the absorption coefficient. The 71.9 gL^{-1}-NaCl solution used in this study has a density of about 1046 gL^{-1} at 20°C. The concentration of water in this solution is therefore 976 g/L, or 54.18M compared to 55.55M for pure water at 20°C. The number of water molecules per volume and, thus, the water absorption coefficient, is reduced by 2.5%. As the density changes with concentration of the solute in a linear manner, the constant value for Ψ_s would be –0.035% g^{-1}L (2.5 / 71.9). This reduction of the absorption coefficient simply by reduction of the number of water molecules per volume is indicated in Fig. 2 as a green line.

No model approach is described for Ψ_S, but it was shown that the spectral features in Ψ_S correlate with the spectral features in the first derivative spectrum of Ψ_T [6]. One theoretical concept for the changes in water absorption with salt concentration is the existence of two types of species of water that are stable and co-exist in the solution, pure water and salt-solvated water [21], each with different absorption coefficient spectra, as the two types have slightly different frequencies for the three fundamental vibrations and the librations. As the concentration of salt-solvated water directly depends on the concentration of the salt ions, the change in the total water absorption is linear with the salt concentration. Pure salt-solvated water was not observed under saturation, but its absorption spectrum was determined for different salts by extrapolation techniques [21]. In addition to these changes, the volume replacement of water molecules by non-absorbing ions reduces the water absorption coefficient equally and linear with the salt concentration - note that this was corrected in [21]. The Ψ_S spectrum is, hence, the sum of these two physical-chemical changes induced by the presence of any ion in water. These results for Ψ_S can be combined with the data of Ψ_S calculated from FTIR measurements at 2600 – 14000 nm [21] (Fig. 2). A full Ψ_S spectrum was thereby constructed for 400 to 14000 nm [see Media 2].

5. Conclusions

The temperature and salinity correction coefficient of the water absorption coefficient, Ψ_T and Ψ_S, were determined for the visible to infrared spectral region of 400 – 14000 nm (wavenumbers: 25000 – 700 cm^{-1}). The newly measured data in the range 400 – 2600 nm agreed well with previously reported values, but provide more precise data for the shortest wavelengths (< 900 nm), and new data for parts of the infrared region, especially for Ψ_S. For Ψ_S we recommend using the data for the ASW at wavelengths > 500 nm, assuming that these values are closer to that of natural seawater than data for a NaCl solution. Below 500 nm, Ψ_S is potentially not significantly different from zero for measurements with current levels of precision.

Acknowledgments

We especially thank Jean-Joseph Max for providing the spectral data of absorption of water and salt solutions, and for his general support. The work was conducted in the framework of the ESA-STSE project *WaterRadiance* (ESTEC Contract No.22192/09/NL/CT).

#220552 - $15.00 USD Received 19 Aug 2014; revised 24 Sep 2014; accepted 24 Sep 2014; published 7 Oct 2014